



## RESEARCH ARTICLE OPEN ACCESS

# Genomic and Ecological Flexibility Shape the Global Distribution of a Black Fungus

Claudia Coleine<sup>1</sup> | Federico Biagioli<sup>2</sup> | Tadeo Sáez-Sandino<sup>3</sup> | Cene Gostinčar<sup>4</sup> | Silvia Turco<sup>5</sup> | Lucia Muggia<sup>6</sup> | Claudio Donati<sup>7</sup> | Alessandro Cestaro<sup>7,8</sup> | Tania Kurbessoian<sup>9</sup> | Eleonora Egidi<sup>3</sup> | Jason E. Stajich<sup>9,10</sup> | Leho Tedersoo<sup>11</sup> | Manuel Delgado-Baquerizo<sup>1</sup>

<sup>1</sup>Laboratorio de Biodiversidad y Funcionamiento Ecosistémico, Instituto de Recursos Naturales y Agrobiología de Sevilla (IRNAS), Consejo Superior de Investigaciones Científicas (CSIC), Seville, Spain | <sup>2</sup>Department of Ecological and Biological Sciences, University of Tuscia, Viterbo, Italy | <sup>3</sup>Hawkesbury Institute for the Environment, Western Sydney University, Penrith, New South Wales, Australia | <sup>4</sup>Biotehniška Fakulteta, Univerza v Ljubljani, Ljubljana, Slovenia | <sup>5</sup>Dipartimento di Scienze Agrarie e Forestali, Università Degli Studi Della Tuscia, Viterbo, Italy | <sup>6</sup>Department of Life Sciences, University of Trieste, Trieste, Italy | <sup>7</sup>Research and Innovation Centre, Fondazione Edmund Mach, San Michele all'Adige, Italy | <sup>8</sup>Bioenergetics and Molecular Biotechnologies (IBIOM), National Research Council (CNR), Institute of Biomembranes, Bari, Italy | <sup>9</sup>Department of Microbiology and Plant Pathology, Institute for Integrative Genome Biology, University of California, Riverside, California, USA | <sup>10</sup>Institute for Integrative Genome Biology, University of California, Riverside, California, USA | <sup>11</sup>Institute of Ecology and Earth Sciences, University of Tartu, Tartu, Estonia

**Correspondence:** Claudia Coleine ([claudia.coleine@irnas.csic.es](mailto:claudia.coleine@irnas.csic.es))

**Received:** 16 October 2025 | **Revised:** 30 March 2026 | **Accepted:** 31 March 2026

**Keywords:** adaptation | extreme-tolerance | global soils | PacBio sequencing | whole-genome sequencing

## ABSTRACT

Black fungi are among the most stress-resistant organisms known, yet the genetic and ecological foundations of their extraordinary resilience remain poorly understood. This study explores the adaptation strategies of the melanised fungus *Elasticomyces elasticus* by integrating genomic and ecological data. To uncover the mechanisms of adaptation, we combined whole-genome sequencing, functional annotation, environmental metadata, and large-scale soil metabarcoding analyses. Phylogenomic approaches were employed to delineate evolutionary lineages and assess ploidy levels. The results revealed that the global distribution of *Elasticomyces* phylotypes is primarily influenced by temperature, UV radiation, and soil organic carbon, suggesting that different phylotypes have evolved heterogeneous strategies for stress resistance. Comparative genomic analyses identified a set of 'sentinel pathways,' notably glutathione metabolism and nucleotide biosynthesis, which were enriched in strains inhabiting the most extreme environments and showed significant correlations with abiotic stressors such as aridity and UV exposure. Furthermore, phylogenomic reconstructions uncovered two independent diploid lineages associated with the harshest environments, pointing to diploidisation as a potential adaptive mechanism to cope with multiple stressors. Overall, the integration of genomic and ecological perspectives provides new insights into how black fungi persist at the edge of habitability. The study highlights specific pathways and genomic traits that underpin resilience to extreme conditions, offering implications that extend beyond terrestrial ecology.

## 1 | Introduction

Highly melanised ascomycetes, also known as microcolonial, meristematic, or rock-inhabiting fungi (RIF), stand out for their ability to colonise hostile environments such as cold deserts, exposed mountain rocks, acid mine drainages, saline sites, and artificial surfaces

(Sterflinger et al. 2012; Coleine, Stajich, and Selbmann 2022; Gostinčar et al. 2024). Mostly from the Dothideomycetes, Eurotiomycetes, and Arthoniomycetes, they share traits such as thick melanised cell walls, meristematic growth, slow metabolism, and production of protective molecules (e.g., mycosporines, trehalose, carotenoids), enabling tolerance to UV and ionising radiation,

This is an open access article under the terms of the [Creative Commons Attribution-NonCommercial](https://creativecommons.org/licenses/by-nc/4.0/) License, which permits use, distribution and reproduction in any medium, provided the original work is properly cited and is not used for commercial purposes.

© 2026 The Author(s). *Environmental Microbiology* published by John Wiley & Sons Ltd.

desiccation, oxidative stress, and temperature extremes (Coleine and Selbmann 2021; Casadevall et al. 2017; Campana et al. 2022; Aureli et al. 2023; Coleine et al. 2024). Notable examples of extremotolerant black fungi include *Cryomyces antarcticus*, capable of withstanding cosmic radiation, desiccation, and simulated Mars conditions (Gomez-Gutierrez et al. 2024); *Exophiala dermatitidis*, commonly found in saunas, dishwashers, and human infections (de León et al. 2025); and *Hortaea werneckii*, a halophilic fungus used as a model for osmotolerance (Busch and Vargas-Muñiz 2025). These organisms challenge conventional limits of habitability and provide critical insights for disciplines as diverse as astrobiology, biotechnology, and evolutionary ecology (Rampelotto 2010; Schultz et al. 2023). Unfortunately, the genetic and ecological traits behind their huge capacity to adapt to polyextreme environments remain poorly understood.

Current uncertainties on the environmental determinants shaping the global biogeography, ecological preferences, and functional diversity of these extremotolerant organisms persist for three main reasons. First, while there is a broad assumption that all black fungi are highly resistant to stress, the reality is that a compressive investigation on the drivers of contrasting black fungi phylotypes is largely lacking. Second, current investigations on black fungi focus on particular aspects of their life styles, ecologies or genomes. Yet, a multidimensional investigation on the contribution of genetic, ecological and phylogenetical drivers in explaining the distribution of these organisms is missing. Finally, while most studies focused on particular locations subject to polyextreme environments (e.g., Antarctica), a global-scale perspective across contrasting climates and vegetations is lacking limiting our capacity to understand the global distribution of these organisms and their overall capacity to withstand stress. This knowledge is key to provide novel understanding on how microbes adapt to a wide range of contrasting environments.

To address these knowledge gaps, we adopted a dual-scale, integrative approach. First, we provide a global overview of the species *Elasticomyces elasticus*, a fungus of particular interest. While it was originally isolated from Antarctic rocks, subsequent records from other continents and substrates, such as soil and lichen thalli, suggest a wider distribution and capabilities to adapt to a broad range of environments (Egidi et al. 2014; Cometto et al. 2023; Coleine et al. 2024). We used long-read amplicon sequencing by Pacific Biosystems (PacBio) technology of topsoils across a wide range of terrestrial biomes. Subsequently, we performed whole-genome sequencing and comparative analyses on a set of *E. elasticus* strains, isolated from various environments and substrates and maintained in culture collections. This approach enables us to investigate how genomic and functional variability among strains reflect adaptation to local environmental pressures, including differences in temperature regimes, UV radiation, and substrate characteristics.

## 2 | Methods

### 2.1 | Global Soils Dataset

Our survey used the GSMc (Global Soil Mycobiome consortium; <https://GSMc-fungi.github.io/>; Tedersoo et al. 2021) dataset to examine the distribution of *E. elasticus* at a global scale. This

dataset consists of highly accurate long-read sequencing of ITS and 18S-V9 variable regions sequenced by PacBio technology, from 128,000 soil sub-samples covering 3200 different localities, across 108 countries in all continents. We assembled our dataset by retrieving relative abundances, taxonomic identification and metadata from the GSMc dataset (Tedersoo et al. 2021), drawing each single Operational Taxonomic Units (OTU) that matched with the considered species. OTU assignment was performed using full-length ITS sequences; dereplicated reads were mapped to OTUs using VSEARCH at 98% sequence similarity, following the workflow described in Tedersoo et al. (2021). The number of reads assigned to each OTU in a given sample was used as a proxy for its relative abundance, calculated relative to all other reads in that sample.

### 2.2 | Environmental Variables Selection

The sample geographic coordinates provided within the GSMc metadata were used to retrieve bioclimatic variables (i.e., MAT, mean annual temperature; TSEA, temperature seasonality; MDR, mean diurnal temperature range; MAP, mean annual precipitation; PSEA, precipitation seasonality) from Worldclim database v. 2.0 (Fick and Hijmans 2017). Data on aridity index (AI) were calculated using the Global Aridity Index and Potential Evapotranspiration (ET0) Database (Zomer et al. 2022). Geographical information about elevation and slope was obtained from the Advanced Land Observation Satellite (ALOS). UV radiation (UV light) was retrieved from NASA satellites (Aura Surface UVB Irradiance, while Human Influence Index (HII)). Other important edaphic drivers of fungal biogeography, such as pH, soil organic carbon (SOC), and sand percentage (Sand%) were also included from SoilGrids (<https://soilgrids.org/>).

Detailed information on the samples with their bioclimatic models can be found in Table S1.

### 2.3 | Statistical Analysis and Present Projections

For comparing and exploring the composition and distribution of *E. elasticus*, the relative abundance of each OTU was estimated using single samples as replicates within the same locality investigated. Then, to get insights on biogeographic and climatic patterns and predict the contribution of environmental factors in driving the distribution of this species, we used the relative abundance data to perform multivariate analysis. To ensure the reliability of statistical inference in redundancy analysis (RDA) and species richness mapping, the variance inflation factor (VIF) was calculated to check the multicollinearity among the environmental variables evaluated. Variables with VIF > 5 were discarded from the regression models (Rillig et al. 2023). Further, for RDA analysis the environmental variables were normalised using Zero Mean and Unit Variance Normalisation, and ‘forward selection’ was used to remove the non-significant predictors from the model. All tests applied were statistically validated by the Benjamini–Hochberg (FDR) *p* value correction method. Analyses were performed using R packages: phyloseq (McMurdie and Holmes 2013) and microeco (Liu et al. 2021).

We then used a machine learning Random Forest (RF) regression analysis (Breiman 2001) in R environment to predict the global distribution of *E. elasticus* in global soils. We used 8 environmental variables, selected for their lack of collinearity, as raster layers using the 'raster' package (Hijmans 2023). For predictive modelling, we implemented a RF algorithm via the 'randomForest' package (Liaw and Wiener 2002), employing an ensemble of 999 decision trees with 100 bootstrap replicates. This configuration optimises model performance while minimising overfitting. To evaluate the precision of the predictions generated by the random forest model, we then measured how much the parameter space of the predictors differed from the original dataset. We created a visualisation mask using Mahalanobis distance analysis to display the most reliable predictions. This mask (based on Mahalanobis distance) incorporates: (1) the distance from each multidimensional point to the centre of the known distribution we previously calculated, and (2) the distance from points representing model training locations. Outliers beyond the 0.95 quantile of the chi-squared distribution (11 degrees of freedom; Mallavan et al. 2010) were masked. Using this outlier identification approach, we visualised only the most reliable predictions ( $\leq 0.95$  chi-squared quantile). Finally, we validated the modelling approach by plotting predicted values ( $x$  axis) against observed values ( $y$  axis, Piñeiro et al. 2008). This procedure allows us to explicitly identify and exclude areas where environmental conditions fall outside the multivariate range of the training data, thereby limiting unreliable extrapolation and ensuring that model projections are restricted to environmentally comparable regions.

## 2.4 | Selection of Cultivated Strains

For the study, 16 strains of *E. elasticus* were selected from two collections: (i) the Culture Collection of Fungi from Extreme Environments (CCFEE) and (ii) CCFEE of the Mycological Section of the Italian National Museum of Antarctica (MNA-CCFEE), <https://antarcticdatacenter.mna.it/srv/api/records/7bf05aae-eb12-4557-b7bc-90b401d1135d>. The strains were chosen to represent various extreme habitats, with an emphasis on fungi isolated from polar and montane rocky environments (Figure 1 and Table S2).

## 2.5 | DNA Extraction and Genome Sequencing

Pure cultures were grown on 2% malt extract agar (MEA) medium plates for 8–10 weeks at 15°C. DNA was extracted from the total biomass following cetyltrimethylammonium bromide (CTAB) protocol, according to Coleine et al. (2024). Melanin was removed through two phenol-chloroform purification steps before DNA extraction. Genomic DNA was sheared with a Covaris S220 ultrasonic homogeniser, and a sequencing library was constructed using the Kapa HyperPlus kit coupled with the KAPA Unique Dual Index adapters (Roche), following the instructions of the manufacturers. Sequencing libraries were prepared using the Nextera DNA Flex Library Preparation Kit (Illumina, CA, USA), following the manufacturer's guidelines. Sequencing was performed on the Illumina NovaSeq 6000 platform, following manufacturer's protocols. All genomes analysed in this study

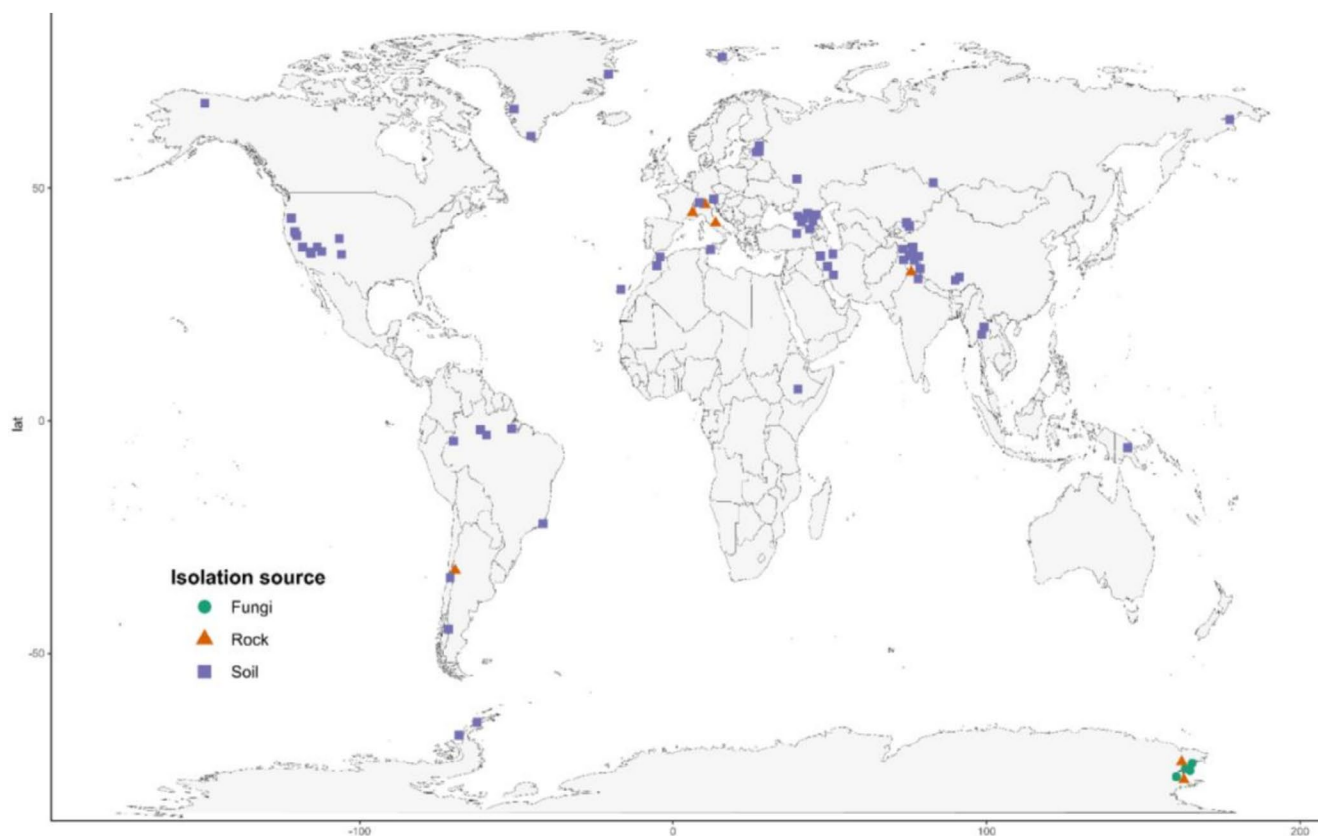


**FIGURE 1** | Global geographic distribution of *Elasticomyces elasticus* isolates and associated sample types. Symbols indicate the isolation source: fungal strains (circles), rock samples (triangles) and soil samples (squares).

were sequenced and assembled exclusively from Illumina short-read data.

All genome sequences analysed in this study were previously generated and published in Coleine et al. (2024) as part of a class-wide comparative genomic survey of black fungi, which included whole-genome sequencing of more than 100 strains (Tables S3 and S4). In the present study, we specifically focused on a subset of those genomes belonging to *E. elasticus* in order to integrate genomic information with global environmental meta-data and soil metabarcoding data.

## 2.6 | Genomes Assembly, Gene Prediction, and Functional Annotation

All genomes were de novo assembled as reported in Coleine et al. (2024). Briefly, the assembly was performed with the AAFTF pipeline v.0.2.3 (Palmer and Stajich 2022), which performs read quality control and filtering with BBTools bbdud v.38.86, followed by SPAdes v.3.15.2 (Bankevich et al. 2012) assembly using default parameters. The BUSCO ascomycota\_odb10 database (Manni et al. 2021) was used to determine genome completeness. Genes in each near-complete genome were annotated with Funannotate v1.8.1. To predict genes, ab initio gene predictors SNAP v.2013\_11\_29 (Korf 2004) and AUGUSTUS v.3.3.3 were used along with additional gene models by GeneMark.HMM-ES v.4.62\_lic (Brůna et al. 2020), and GlimmerHMM v.3.0.4 (Majoros et al. 2004) utilise a self-training procedure to optimise ab initio predictions. Finally, EvidenceModeler v.1.1.1 (Haas et al. 2008) generated consensus gene models in Funannotate that were constructed using default evidence weights. Non-protein-coding tRNA genes were predicted by tRNAscan-SE v.2.0.9 (Chan and Lowe 2016). Putative protein functions were assigned to genes based on sequence similarity to the Interpro database. EggNOG v.5 (Huerta-Cepas et al. 2017) was used to obtain KEGG functional orthologs (Kanehisa et al. 2014) (Table S5).

Orthologous proteins were then identified using OrthoFinder v2.5.5 (Emms and Kelly 2019), and the results were processed further using the R package UpsetR v1.4 (Conway et al. 2017) within the R environment (v4.2.3). The species tree built by OrthoFinder was visualised in a dendrogram using FigTree v1.4.4 (<http://tree.bio.ed.ac.uk/software/figtree/>) and further edited with Inkscape v0.92 (<https://inkscape.org>).

## 2.7 | Genomes Statistical Analysis

Functional genomic profiles were inferred from KEGG ortholog annotations obtained using eggNOG-mapper. For each genome, the number of genes assigned to each KEGG ortholog (KO) was quantified and subsequently aggregated at the pathway level, generating a genome-by-pathway abundance matrix. These pathway abundances were used as proxies of functional genomic potential rather than as measures of metabolic completeness or physiological performance. Prior to statistical analyses, pathway counts were normalised by total annotated genes per genome to account for differences in assembly size and gene number. The resulting normalised

pathway matrix was then used in correlation analyses and Random Forest models to identify associations between functional genomic profiles and environmental variables at the sites of strain isolation.

We used the Random Forest model to identify the major significant environmental predictors explaining the variation of metabolic competences in black fungi according to environmental variables. The importance of each predictor variable is determined by evaluating the decrease in prediction accuracy, that is, increase in the mean square error between observations and OOB (out-of-bag) predictions, when the data for that predictor is randomly permuted. RF was implemented using the 'randomForest' package v.4.6–14 in the R environment.

We then used one-by-one Spearman correlation analysis concurrently with RDA to identify the most important environmental factors in driving the biogeographic and climatic patterns of *E. elasticus* phylotypes, using the 'microeco' R package. To ensure the reliability of statistical inference in RDA analysis, the VIF was calculated to check the multicollinearity among environmental variables evaluated. Variables with VIF > 5 were discarded from the RDA model.

While the previous analyses focused on OTU-level abundance patterns derived from global soil metabarcoding data, the following analyses specifically investigate genome-derived functional profiles of cultivated strains in relation to the environmental conditions at their sites of isolation.

## 2.8 | Genome Ploidy Analysis

The genome assemblies were aligned with Sibeliaz v.1.2.5 (Minkin and Medvedev 2020) using the options '-k 21 -a 150 -b 15000'. Only alignments with 14 to 29 sequences were kept and converted to multi-fasta alignments. Genomes from CCFEE strains 5506, 5537, 5810, 5806, 5966, 5805 were represented by an average of 5280 sequences (SD 36) and genomes 5544, 5543, 5316, 5320, 5319, 5313 were represented by an average of 10,703 sequences (SD 118). The genomes 5474, 6128, and 5547 were removed from the dataset due to a large amount of missing data. We kept only alignments with 18 sequences (corresponding to the expected number for 6 haploid and 6 diploid genomes). The length of gap-free alignments was calculated with Gblocks 0.91b (options '-t=p -b3 = 10 -b4 = 3 -b5 = n -p = n') (Castresana 2000) and infoalign (part of EMBOSS:6.6.0.0) (Rice et al. 2000). Phylogenetic trees were calculated from each of the longest 100 alignments (not processed with Gblocks), together representing a total of 1,805,911 gapless alignment length. IQ-TREE 2.0.3 with 1000 replicates of SH-like approximate likelihood ratio test (SH-aLRT) was used, with automatic estimation of the best nucleotide substitution model (Nguyen et al. 2015). The names of sequences in the phylogenies were shortened to strain names, thus producing multi-labelled trees. The collection of all 100 trees was imported into the R environment and differences between trees were calculated with the DifferentPhylogeneticInfo function provided by the package TreeDist (Smith 2020). The resulting matrix of differences was used to estimate the optimal number of clusters with fviz\_nbclust(), part of package factoextra

(Kassambara and Mundt 2020), using kmeans and ‘silhouette’ method. The clustering itself was performed with *pam* function, part of the *cluster* package and the representative tree of each of the three clusters determined as the medoid of the cluster (<https://cran.r-project.org/web/packages/cluster/citation.html>). Representative trees were visualised in Dendroscope (Huson et al. 2007) and labels added in Inkscape.

### 3 | Results

#### 3.1 | Global Soil Distribution and Environmental Predictors of *E. elasticus*

The GSMc dataset (Tedersoo et al. 2021) was used in our survey to retrieve *E. elasticus* sequences. This dataset provides an extensive library comprising more than 722,000 fungal OTUs. To identify the OTUs belonging to *E. elasticus*, we filtered the original taxonomic table provided by Tedersoo et al. (2021), retaining at species level only those OTUs ( $n = 53$ ) assigned to *E. elasticus*.

Analysis of the distribution of *E. elasticus* revealed that most OTUs were more frequently found in temperate soils, followed by arid, continental, and polar/montane environments (Figure 2A). A random forest (RF) model was applied to assess the importance of environmental variables in explaining the global occurrence and abundance of this species. The results showed that mean annual temperature (MAT) and elevation were the most influential predictors ( $p < 0.001$ ), followed by soil organic carbon (SOC) ( $p < 0.01$ ) and aridity index (AI) ( $p < 0.05$ ) (Figure 2B).

#### 3.2 | Contrasting Environmental Preferences Within *E. elasticus*

To reveal if *E. elasticus* phylotypes can adapt to very different environments, multivariate ordination via RDA. This analysis revealed that the community composition of *E. elasticus* is significantly structured along key environmental gradients (Figure 3A). Among the abiotic variables, elevation, soil pH, and mean annual temperature (MAT) exerted the strongest directional influence on the distribution of OTUs. In particular, a few strains grouped closely along the elevation axis, suggesting they may represent cold-adapted taxa potentially restricted to alpine or montane soils. Conversely, OTU43, OTU41, and OTU23 were aligned against the vectors of SOC (soil organic carbon) and aridity index (AI), indicating they may be stress-tolerant or oligotrophic taxa favoured in dry, carbon-poor environments. These patterns were corroborated by a correlation-based approach (Figure 3B). OTU39 displayed highly significant positive correlations with elevation ( $p < 0.001$ ), and to a lesser extent with UV exposure and terrain slope, pointing to a possible adaptation to high-altitude, high-irradiance soils. Notably, OTU39 was negatively correlated with temperature, suggesting a strong preference for cold conditions. OTUs 2, 8, OTU23, 35, and 47 were associated with arid environments, hinting at possible xerotolerance or photo-protection strategies.

#### 3.3 | Global Distribution Model of *E. elasticus*

The current species distribution model (SDM) for *E. elasticus*, based on environmental niche modelling and soil fungal

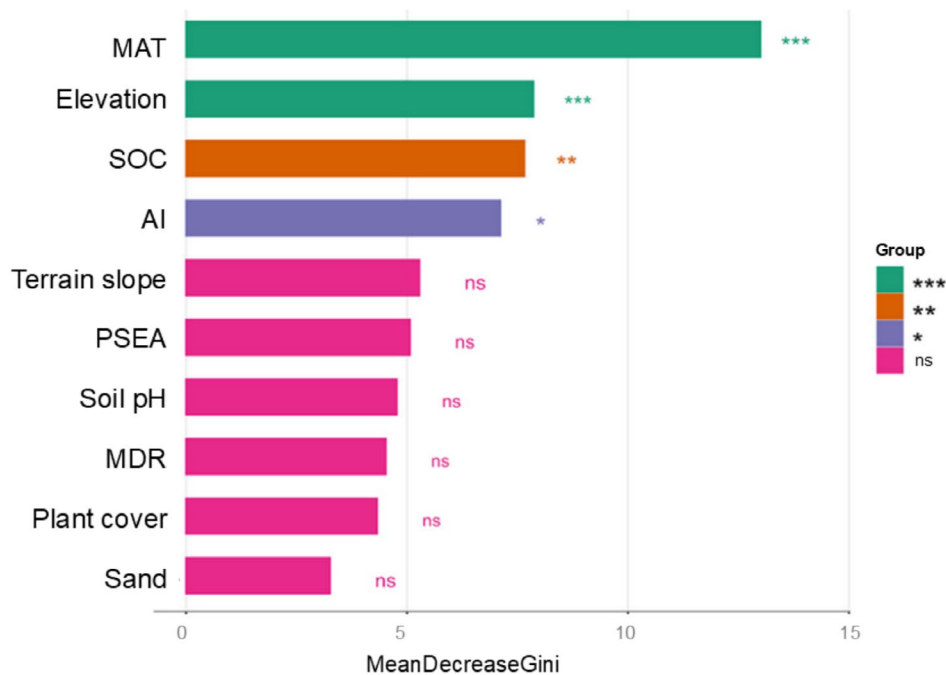


**FIGURE 2** | Environmental drivers of *Elasticomyces elasticus*. Importance of environmental predictors for explaining functional genomic diversity in *E. elasticus*, based on Random Forest analysis. Mean decrease in Gini index is used to rank predictor variables. Asterisks indicate level of significance (\* $p < 0.05$ , \*\* $p < 0.01$ , \*\*\* $p < 0.001$ ). AI, aridity index; MAT, mean annual temperature; MDR, mean diurnal range; PSEA, precipitation seasonality; SOC, soil organic matter.

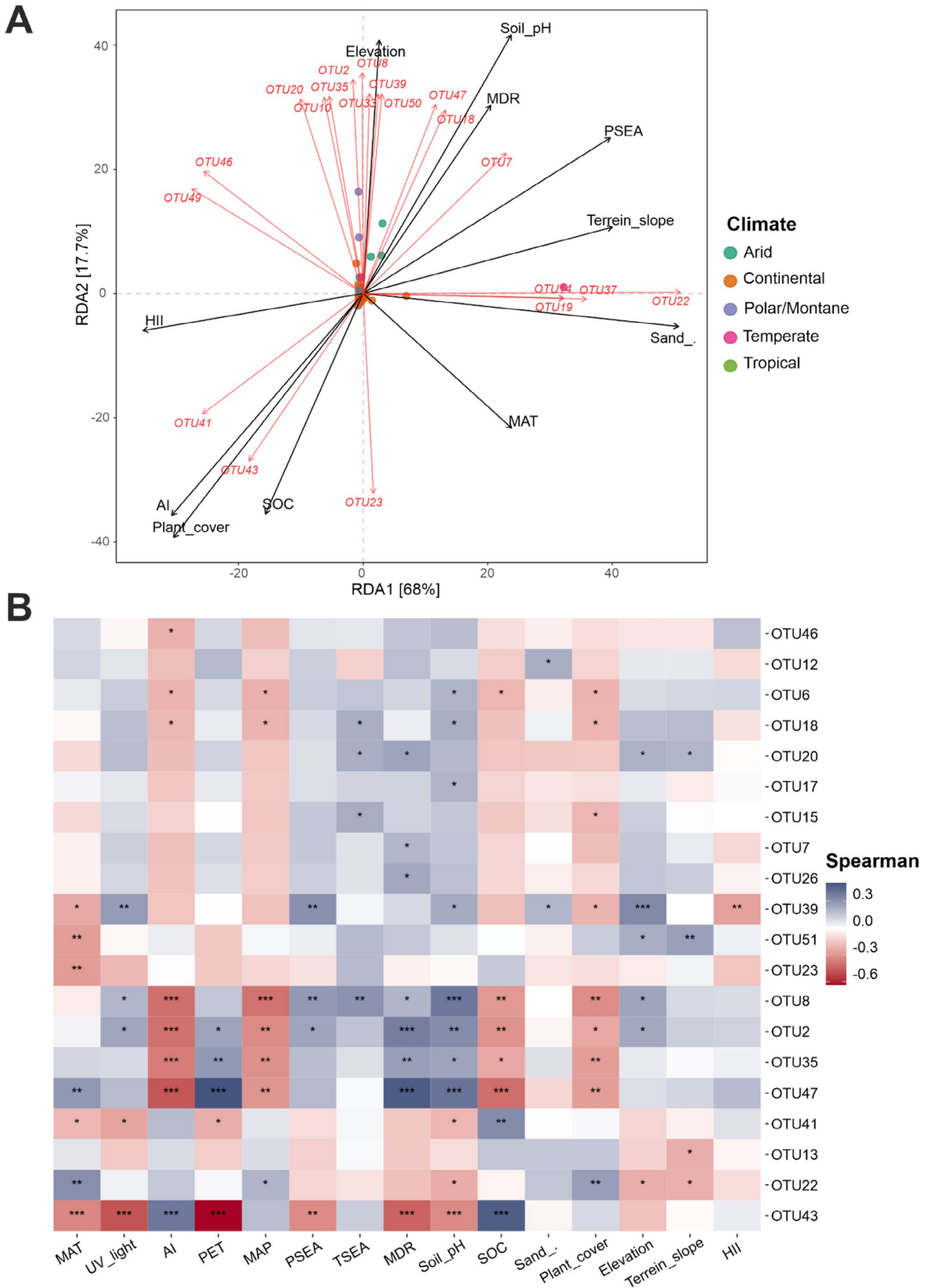
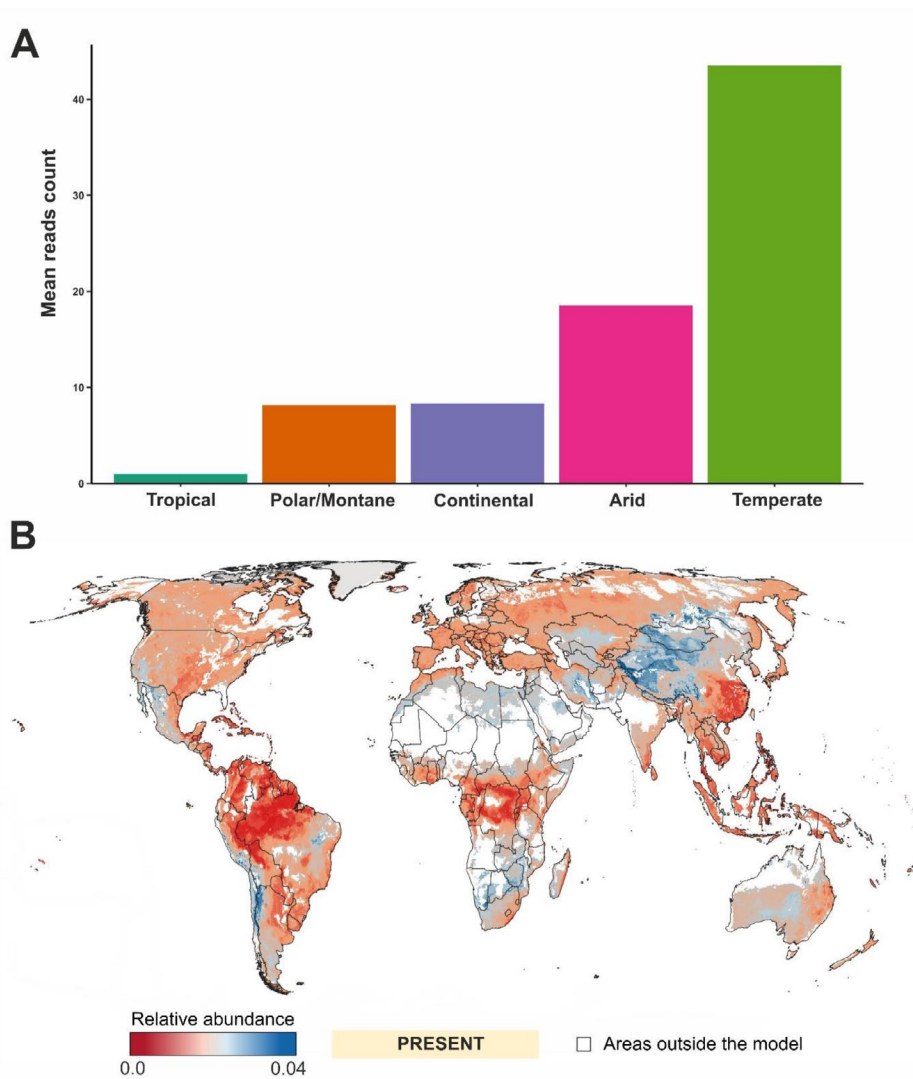


FIGURE 3 | Legend on next page.

**FIGURE 3** | (A) Redundancy analysis (RDA) triplot showing the relationship between environmental variables (black arrows), fungal OTUs (red vectors), and sample categories (coloured dots). The ordination reveals that specific fungal taxa are associated with distinct environmental gradients, particularly with elevation. (B) Heatmap of Spearman correlations between the relative abundance of selected fungal OTUs and environmental parameters. Blue and red colours indicate positive and negative correlations, respectively. Asterisks denote statistical significance (\* $p < 0.05$ , \*\* $p < 0.01$ , \*\*\* $p < 0.001$ ). AI, aridity index; HII, human influence index; MAT, mean annual temperature; MDR, mean diurnal range; PET, potential evapotranspiration; PSEA, precipitation seasonality; SOC, soil organic carbon; TSEA, temperature seasonality; UV light, ultraviolet light radiation.



**FIGURE 4** | Distribution of *Elasticomyces elasticus*. (A) Relative abundance of *Elasticomyces elasticus* sequences retrieved from PacBio samples across major climatic regions. (B) Projected current global distribution of *Elasticomyces elasticus* based on environmental niche modelling. Colours represent relative abundance predicted from soil environmental variables and known occurrence points, with blue indicating higher abundance and red indicating lower suitability. These projections are based on species distribution models incorporating key climatic variables, including slope, mean annual temperature (MAT), mean annual precipitation (MAP), Normalised Difference Vegetation Index (NDVI), soil organic carbon (SOC), mean diurnal range (MDR), fine texture, and precipitation seasonality (PSEA).

metabarcoding data, reveals a heterogeneous but distinct global pattern of relative abundance (Figure 4A). The model projects higher predicted abundance (blue regions) in key areas such as the Tibetan Plateau, Central Asia, the southern Andes (e.g.,

Chile), parts of eastern Africa, and southern Australia. These regions are characterised by medium-to-high soil organic content and moderate-to-low temperature, aligning with the key predictors identified in our RF analysis (Figure 4B).

### 3.4 | Survival Strategies and Functional Genomic Traits Along Environmental Gradients

Once we have a better understanding of the ecology of *E. elasticus*, we seek to explore the genetic traits associated with these environments aiming to provide new insights into how they survive to such conditions. We first summarised orthogroup overlap among isolates from Argentina, Italy, India and Antarctica using an UpSet representation (Figure 5A). This analysis revealed a large core genome composed of 11,450 orthogroups shared across all geographic origins, representing a conserved functional ‘core’ of *E. elasticus*. Beyond this core fraction, the pangenome showed a structured accessory component, with several thousand orthogroups shared among subsets of genomes from three geographic regions (e.g., 1593 and 446 orthogroups) or between pairs of regions (e.g., 4292 orthogroups), indicating partial geographic specificity. In addition, a smaller number of orthogroups were restricted to single geographic origins or individual strains, representing country-specific and strain-specific gene content (singletons) (Table S6). Together, these patterns indicate that *E. elasticus* combines a highly conserved core gene set with a flexible accessory genome, suggesting that while core functions are

maintained across environments, a variable fraction of the genome may contribute to local adaptation.

Guided by the overlap structure, we related KEGG-mapped functional profiles to predictors that capture radiation and water/energy balance (UV exposure, mean annual precipitation—MAP, temperature, elevation, aridity index) plus SOC. We combined correlation analyses with model-based importance scores to identify pathways consistently associated with environment (Figure 5B).

For example, pathways associated with nucleotide metabolism purine (KEGG:map00230) and pyrimidine (KEGG:map00240) were positively correlated with UV exposure. Climate also showed a clear genetic signature associated with these organisms. For instance, MAP showed negative correlations with pathways including the RIG-I-like receptor signalling (map04622) and apoptosis (map04215). The observed depletion of biosynthetic pathways like staurosporine (KEGG:map00404) and diterpenoid metabolism (KEGG:map00904) under high MAP suggests that secondary metabolic adaptations, often associated with oxidative stress and signalling, are favoured in dry, oligotrophic niches.

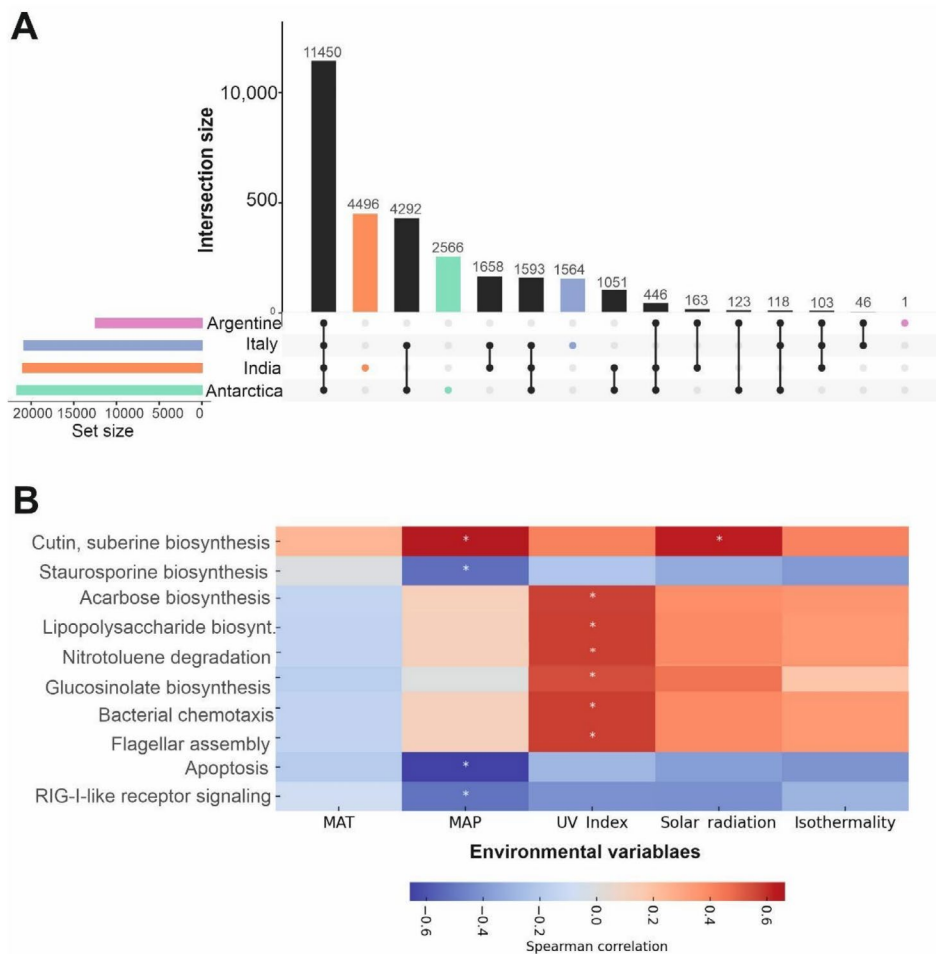


**FIGURE 5** | Functional biogeography and environmental associations of genomic traits in *Elasticomyces elasticus*. (A) UpSet plot showing the intersections of predicted orthogroups among *E. elasticus* genomes grouped by geographic origin. (B) Heatmap of Spearman correlations between the relative abundance of KEGG pathways and environmental variables. Blue tones indicate negative associations; asterisks denote statistical significance ( $p < 0.05$ ). AI, aridity index; MAT, mean annual temperature; MDR, mean diurnal range; PSEA, precipitation seasonality.

Notably, isothermality, a measure of diurnal thermal variability, showed no significant correlations, suggesting that *E. elasticus* adaptation may not be strongly driven by short-term thermal fluctuations.

### 3.5 | Phylogenetic Structure Reveals Independent Diploidisation Events in *E. elasticus*

The phylogenetic reconstruction of *E. elasticus* strains based on whole-genome alignment reveals a robust clustering pattern that reflects ploidy state (Figure 6). Genome ploidy was inferred based on whole-genome syntenic alignments, where diploid genomes were identified by the systematic presence of approximately two homologous sequences per genomic region across conserved syntenic blocks. Clustering of these trees via k-means and silhouette methods identified three phylogenetically stable groups: two composed exclusively of diploid strains, and one comprising haploid strains and basal lineages. The consistent recovery of the two diploid clades across all trees supports the occurrence of at least two independent diploidisation events in the evolutionary history of *E. elasticus*. The diploid clades include genomes CCFEE 5313, 5316, 5319, and 5320 (clade A), and another divergent cluster (CCFEE 5543, 5544—clade B), with non-sister relationships across topologies, reinforcing the view of convergent genome duplication.

## 4 | Discussion

Our integrative study combining genomic and ecological data demonstrates that *E. elasticus* phylotypes are not uniformly polyextremotolerant but rather exhibit a broad spectrum of environmental sensitivities and adaptive strategies. While some lineages thrive in harsh conditions, others may be more

vulnerable to environmental change. In this case, the global distribution is best predicted by macroclimatic and edaphic factors such as mean annual temperature (MAT), elevation, aridity, and soil organic carbon. These variables define broad-scale habitat suitability, suggesting that thermal and energetic constraints, rather than microhabitat features, govern the species' global prevalence.

The biogeographic pattern of *E. elasticus* partially overlaps with other melanised fungi such as *Exophiala* and *Cladophialophora*, yet diverges in key ecological drivers. While the latter taxa are more influenced by UV radiation, precipitation seasonality, and soil structure (Coleine, Selbmann, et al. 2022), *E. elasticus* appears to be shaped more strongly by temperature and elevation gradients. These ecological contrasts likely reflect different evolutionary trajectories: *E. elasticus*, a Dothideomycete, emerged in the late Devonian, a much cooler period than the Triassic, when Chaetothyriomycetes such as *Exophiala* diversified. Indeed, phylogenetic and molecular dating analyses indicate that rock-inhabiting lineages within Dothideomyceta originated during the late Devonian, a period characterised by extensive arid landmasses, relatively cooler climates compared to the Triassic, and widespread oligotrophic rocky substrates, conditions that likely promoted early adaptation to stress-prone environments (Gueidan et al. 2011). Dothideomycetes, such as *E. elasticus*, evolved in the late Devonian era, much earlier than Chaetothyriomycetes, which evolved in the Triassic (Gueidan et al. 2011). Nevertheless, both groups of extremophiles originated, radiated and evolved under periods of abiotic stresses and had to adapt their life to nutrient-poor, rocky habitats (Gueidan et al. 2011).

Broader patterns were also observed in global fungal surveys. Studies by Tederloo et al. (2014), Bahram et al. (2018), and Egidi et al. (2019) have shown that Dothideomycetes and other

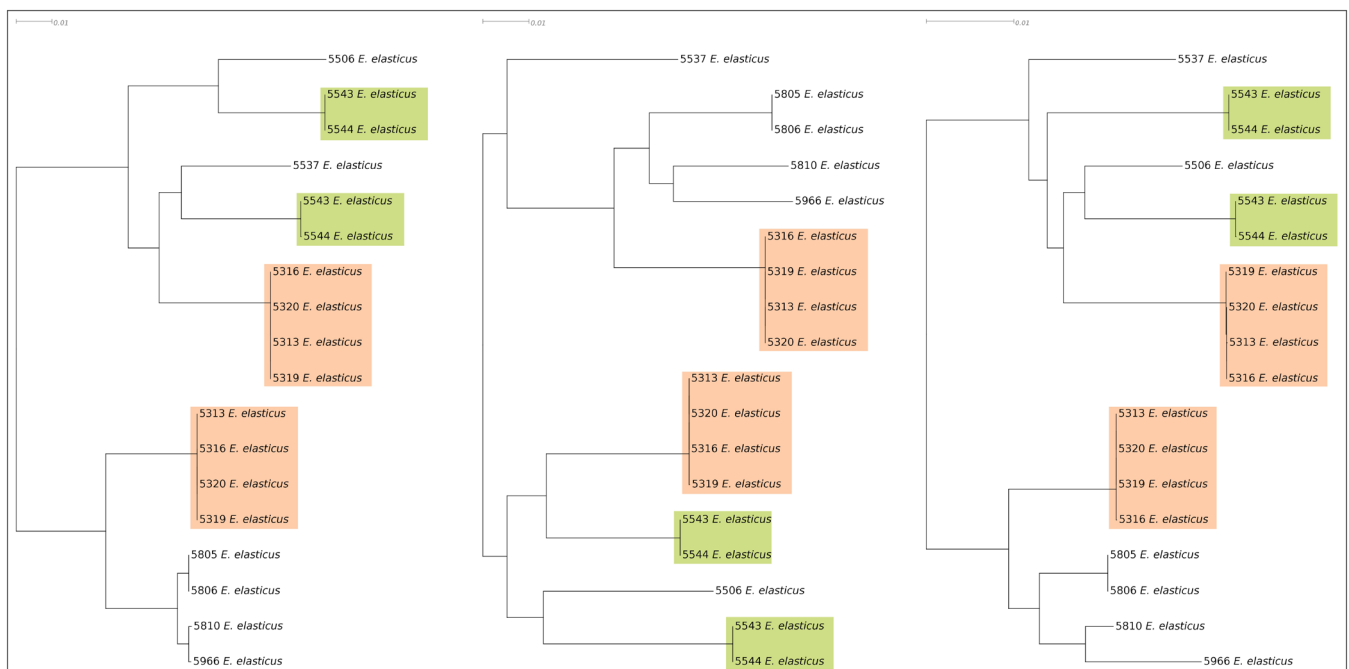


**FIGURE 6** | Phylogenetic reconstruction of *Elasticomyces elasticus* strains based on genomic data, showing three independent analyses. Coloured boxes indicate ploidy groups, that is, diploid strains (orange [clade A] and green [clade B]), whereas uncoloured strains represent haploid lineages.

melanised fungi often dominate xeric, oligotrophic soils across continents. These organisms may be considered ‘ubiquitous specialists’ occurring globally but confined to specific abiotic niches within each biome. This ecological strategy could explain the patchy yet predictable presence of *E. elasticus*, which is favoured in habitats with steep thermal or altitudinal gradients, even when overall climate harshness is moderate. This contrasts with taxa like *Cladophialophora minutissima*, which shows moderate sensitivity to soil pH—an axis less important in our SDM for *E. elasticus* in our analyses (Sterflinger et al. 2012; Coleine et al. 2024).

Our study further reveals that *E. elasticus* phylotypes exhibit considerable ecological flexibility, with some lineages thriving under relatively low-stress conditions and potentially being more vulnerable to environmental change. This challenges the prevailing assumption that black fungi are uniformly adapted to polyextreme environments. These findings suggest that *E. elasticus* is not ecologically uniform, but instead exhibits environmentally associated genetic and functional variation along climatic and edaphic gradients. This ecological divergence could reflect underlying genetic differentiation, possibly corresponding to cryptic, niche-adapted taxa. Alternatively, *E. elasticus* may represent a broadly distributed taxon with high gene flow among populations, maintaining genetic cohesion and intraspecific variability that blurs the emergence of allopatric speciation. Disentangling these possibilities would require further genomic and population-level analyses, beyond the scope of this study.

Such intra-specific ecological divergence mirrors patterns reported in many microbial taxa, where wide geographic ranges conceal hidden functional and ecological complexity. Rather than relying solely on phenotypic plasticity, many of these organisms maintain multiple, locally adapted lineages. For example, Leff et al. (2015) showed that fungal OTUs from the same species complex respond independently to climate and precipitation. Similarly, Purahong et al. (2016) found that even narrow bioclimatic or phylogenetic ranges exhibit strong environmental filtering and long-term habitat conservatism.

Parallel insights from bacterial systems reinforce these observations. Martiny et al. (2015) emphasised that taxonomic resolution often fails to capture ecological differentiation. The concept of ‘cryptic specialisation’ has emerged to describe how apparently ubiquitous taxa survive via functionally distinct sublineages. In fungi, such differentiation may be enhanced by traits like stress-tolerant cell walls, meristematic growth, and slow metabolism, whereby community dynamics and resilience under stress often result from within-taxon functional heterogeneity (Crowther et al. 2014). Further evidence suggests that intra-clade ecological divergence is driven by pH, host identity, and soil chemistry (Rosling et al. 2013; Sato et al. 2017).

The current species distribution model for this species reveals a heterogeneous yet well-defined global pattern of predicted relative abundance. The model highlights regions of high predicted abundance, including the Tibetan Plateau, Central Asia, the southern Andes, parts of eastern Africa, and southern Australia. These regions share common environmental features such as moderate-to-low mean annual temperatures and medium-to-high soil organic carbon content, factors identified

as the strongest predictors of *E. elasticus* occurrence in our random forest analysis.

Notably, several of these areas coincide with the geographic origin of lichen thalli from which *E. elasticus* was previously isolated (Cometto et al. 2023, 2024), supporting the ecological relevance of the modelled distribution. Although tropical regions receive high levels of UV radiation, *E. elasticus* shows low predicted abundance in these zones, likely due to the combined effects of elevated temperatures and high moisture levels, which fall outside the species’ optimal niche. Accordingly, low abundance is projected across most tropical and equatorial areas, including the Amazon Basin, central Africa, and Southeast Asia, suggesting that stable, humid environments with limited soil organic carbon available for decomposition are suboptimal for this extremotolerant fungus. While *E. elasticus* exhibits a truly global distribution, global occurrence alone does not necessarily imply extensive intercontinental gene flow. In many cosmopolitan fungi, broad geographic distributions coexist with limited effective gene flow and pronounced local genetic structuring, reflecting a decoupling between dispersal potential and realised genetic exchange. In the case of *E. elasticus*, sexual reproduction has not been observed, and the mechanisms by which genetic material is exchanged among populations remain poorly understood. Although melanisation and thick cell walls may facilitate long-distance dispersal by enhancing resistance to UV radiation and desiccation, successful dispersal does not necessarily result in effective gene flow if colonising propagules fail to recombine or establish persistent populations. As a result, widespread dispersal of melanised, stress-tolerant propagules may contribute to global occurrence without erasing local genetic structure. Consequently, the relationship between dispersal, reproduction, and gene flow in *E. elasticus* remains an open question that cannot be resolved with the current dataset.

We have also highlighted that environmental gradients such as UV exposure, water availability, and resource constraints exert strong selective pressures on the genomic architecture of *E. elasticus*. By integrating correlation statistics with model-based feature importance, we identified a subset of pathways significantly associated with abiotic conditions. For instance, several functions, critical for DNA synthesis and repair, were positively correlated with UV exposure. Similar patterns have been observed not only in prokaryotes such as *Deinococcus radiodurans* and *Halobacterium salinarum*, both known for their resistance to radiation and desiccation through enhanced nucleotide metabolism and DNA repair mechanisms (Vafadarnejad et al. 2015; Cox et al. 2010; Slade et al. 2009), but also in extremotolerant fungi. For example, melanised taxa such as *C. antarcticus* and other RIF show enhanced DNA repair and protective metabolic responses associated with radiation tolerance and long-term persistence under extreme conditions (Coleine, Stajich, and Selbmann 2022; Coleine, Selbmann, et al. 2022). Interestingly, isothermality, a proxy for diurnal temperature stability, showed no significant genomic correlation. This may indicate that *E. elasticus* is less influenced by short-term thermal fluctuations and instead relies on mechanisms conferring robustness to rapid environmental changes such as desiccation-rehydration cycles. This contrasts with other black fungi, such as Antarctic rocks endemic fungi, which exhibit genomic signatures shaped by long-term stability and niche specialisation (Cary et al. 2010). Aridity also emerged

as a strong predictor of genomic responses. This strategy mirrors responses observed in *Chroococciopsis* spp., radiation-resistant cyanobacteria that suppress apoptosis and invest in antioxidant and repair pathways to persist under extreme dryness and UV radiation (Napoli et al. 2021; Li et al. 2022), as well as in extremophilic fungi such as *H. werneckii*, which exhibit metabolic flexibility and stress-response pathways enabling survival under osmotic stress, desiccation, and high radiation (Gostinčar et al. 2021). More broadly, fungi display a complex and tightly regulated network of programmed cell death (PCD) pathways that can be modulated or attenuated under environmental stress, balancing survival and cell sacrifice depending on ecological context (Gonçalves et al. 2017; Hardwick 2018). In extremophiles, this balance appears shifted toward survival-oriented responses, with suppression or fine-tuning of PCD coupled to enhanced oxidative stress management, mitochondrial regulation, and repair mechanisms, ultimately promoting persistence under chronic environmental pressure rather than activation of canonical death pathways.

The phylogenomic reconstruction of *E. elasticus* strains, based on whole-genome alignments, reveals a robust clustering pattern that reflects ploidy state. Environmental metadata link these diploid strains to polyextreme regions such as Antarctica and the Himalayan Plateau, habitats characterised by extreme cold, intense UV radiation, desiccation, and low nutrient availability. While overall genome sizes are broadly comparable, this altitudinal pattern suggests a link between genome expansion and high-altitude, polyextreme conditions. Together, these observations indicate that genome expansion, partly mediated by diploidisation, may represent a non-random adaptive response to long-term genomic stress, providing redundancy, mutational buffering, and an expanded stress-response repertoire, as proposed for other fungi and plants (Vande Zande et al. 2023; Baduel et al. 2019).

Analogous adaptive ploidy shifts have been documented in several extreme fungi. For example, the halotolerant black yeast underwent whole-genome duplication and hybridisation events, resulting in diploid genomes with enhanced stress-response capacity (Lenassi et al. 2013; Sinha et al. 2017; Gostinčar et al. 2021). Similar trends are observed in other extremotolerant fungi. In *Cryptococcus neoformans*, polyploid titan cells form in response to environmental or host-derived stress, enhancing survival and genomic flexibility (Fu et al. 2021; Vande Zande et al. 2023). Likewise, *Candida albicans* modulates ploidy under antifungal pressure, increasing genetic diversity and adaptive potential (Avramovska and Hickman 2019). Together, these examples support a model in which ploidy variation serves as a reversible and adaptive mechanism enabling fungal survival under environmental stress.

However, genome expansion in extreme environments does not necessarily rely on ploidy shifts alone. In other cold-adapted fungi and plants, including Arctic taxa and fungi such as *Mycena*, increased genome size has been linked to expansion of transposable (TE) and repetitive elements rather than whole-genome duplication (Harder et al. 2024). Such TE-driven expansion has been associated with prolonged phases of genomic vulnerability, including monokaryotic stages with elevated transposable element activity, potentially facilitating rapid adaptation (Baduel

et al. 2019). Together, these observations suggest that genome enlargement, via diploidisation, repeat expansion, or a combination of both, may represent a general adaptive strategy to cope with extreme environments, with different lineages relying on distinct but potentially complementary genomic routes.

## 5 | Conclusions

Our integrative study of the genus *E. elasticus*, combining global environmental metadata, genomic profiling, and metabarcoding data, offers novel insights into the adaptation, ecological and genetic mechanisms of this, not always, poly-extreme fungus to its environment. Phylogenomic analyses reveal at least two independent diploidisation events, each giving rise to distinct clades associated with harshest climatic niches. These findings suggest that genome duplication acts as an adaptive strategy, enhancing stress resilience through gene redundancy and metabolic flexibility. *E. elasticus* thus emerges as a powerful model for understanding how microeukaryotes evolve functional diversity and genome complexity in response to extreme terrestrial conditions. More broadly, our results highlight ploidy shifts, metabolic rewiring, and niche-specific specialisation as central components of eukaryotic adaptation and underscore the importance of integrating comparative genomics with ecological context to forecast microbial resilience under future environmental change.

### Author Contributions

Claudia Coleine conceived the study. All coauthors contributed to conceptualization and data interpretation. Leho Tedersoo generated the PacBio amplicon sequencing datasets. Claudia Coleine, Jason E. Stajich, Tania Kurbessoian, Alessandro Cestaro and Claudio Donati produced the whole-genome sequencing data, assembled and annotated the genomes. Manuel Delgado-Baquerizo has provided environmental metadata. Claudia Coleine, Federico Biagioli, Tadeo Sáez-Sandino, Silvia Turco, Cene Gostinčar, Eleonora Egidi and Lucia Muggia performed analyses and interpreted data. Claudia Coleine wrote the first draft of the manuscript. All coauthors contributed to subsequent versions of the manuscript. All authors read and approved the final manuscript.

### Acknowledgements

C.C. wishes to thank the Italian National Antarctic Research Program (PNRA) for funding sampling campaigns and research activities in Italy in the frame of PNRA projects. The Italian Antarctic National Museum (MNA) is kindly acknowledged for financial support to the Mycological Section of the MNA (University of Tuscia, Italy), where the fungal specimens used in this study are stored.

### Conflicts of Interest

The authors declare no conflicts of interest.

### Data Availability Statement

The GSMc original dataset files including OTU-table, OTU-taxonomy and relative metadata are available from the PlutoF data repository (<https://doi.org/10.15156/BIO/2263453>). The genome assemblies and annotation datasets are available on Zenodo repository (<https://doi.org/10.5281/zenodo.7764743>) and on NCBI SRA under number of accession PRJNA666634. Workflow of statistical analysis is available in Zenodo repository (<https://doi.org/10.5281/zenodo.17153571>). The complete set

of phylogenetic trees and whole-genome alignments generated in this study has been deposited and are publicly available in Figshare (DOI: <https://doi.org/10.6084/m9.figshare.31295908>).

## References

- Aureli, L., C. Coleine, M. Delgado-Baquerizo, et al. 2023. "Geography and Environmental Pressure Are Predictive of Class-Specific Radioresistance in Black Fungi." *Environmental Microbiology* 25, no. 12: 2931–2942.
- Avramovska, O., and M. A. Hickman. 2019. "The Magnitude of *Candida albicans* Stress-Induced Genome Instability Results From an Interaction Between Ploidy and Antifungal Drugs." *G3: Genes, Genomes, Genetics* 9, no. 12: 4019–4027.
- Baduel, P., L. Quadrana, B. Hunter, K. Bombliès, and V. Colot. 2019. "Relaxed Purifying Selection in Autopolyploids Drives Transposable Element Over-Accumulation Which Provides Variants for Local Adaptation." *Nature Communications* 10, no. 1: 5818.
- Bahram, M., F. Hildebrand, S. K. Forslund, et al. 2018. "Structure and Function of the Global Topsoil Microbiome." *Nature* 560, no. 7717: 233–237.
- Bankevich, A., S. Nurk, D. Antipov, et al. 2012. "SPAdes: A New Genome Assembly Algorithm and Its Applications to Single-Cell Sequencing." *Journal of Computational Biology* 19, no. 5: 455–477.
- Breiman, L. 2001. "Random Forests." *Machine Learning* 45, no. 1: 5–32.
- Brůna, T., A. Lomsadze, and M. Borodovsky. 2020. "GeneMark-EP+: Eukaryotic Gene Prediction With Self-Training in the Space of Genes and Proteins." *NAR Genomics and Bioinformatics* 2, no. 2: lqaa026.
- Busch, R. J., and J. M. Vargas-Muñiz. 2025. "*Hortaea werneckii*." *Trends in Microbiology* 33: 1033–1034.
- Campana, R., F. Fanelli, and M. Sisti. 2022. "Role of Melanin in the Black Yeast Fungi *Aureobasidium pullulans* and *Zalaria obscura* in Promoting Tolerance to Environmental Stresses and to Antimicrobial Compounds." *Fungal Biology* 126, no. 11–12: 817–825.
- Cary, S. C., I. R. McDonald, J. E. Barrett, and D. A. Cowan. 2010. "On the Rocks: The Microbiology of Antarctic Dry Valley Soils." *Nature Reviews Microbiology* 8, no. 2: 129–138.
- Casadevall, A., R. J. Cordero, R. Bryan, J. Nosanchuk, and E. Dadachova. 2017. "Melanin, Radiation, and Energy Transduction in Fungi." *Microbiology Spectrum* 5, no. 2: 10–1128.
- Castresana, J. 2000. "Selection of Conserved Blocks From Multiple Alignments for Their Use in Phylogenetic Analysis." *Molecular Biology and Evolution* 17: 540–552.
- Chan, P. P., and T. M. Lowe. 2016. "GtRNAdb 2.0: An Expanded Database of Transfer RNA Genes Identified in Complete and Draft Genomes." *Nucleic Acids Research* 44, no. D1: D184–D189.
- Coleine, C., T. Kurbessoian, G. Calia, et al. 2024. "Class-Wide Genomic Tendency Throughout Specific Extremes in Black Fungi." *Fungal Diversity* 125, no. 1: 121–138.
- Coleine, C., and L. Selbmann. 2021. "2.1 Black Fungi Inhabiting Rock Surfaces." In *Life at Rock Surfaces*, 57–86. De Gruyter.
- Coleine, C., L. Selbmann, B. K. Singh, and M. Delgado-Baquerizo. 2022. "The Poly-Extreme Tolerant Black Yeasts Are Prevalent Under High Ultraviolet Light and Climatic Seasonality Across Soils of Global Biomes." *Environmental Microbiology* 24, no. 4: 1988–1999.
- Coleine, C., J. E. Stajich, and L. Selbmann. 2022. "Fungi Are Key Players in Extreme Ecosystems." *Trends in Ecology & Evolution* 37, no. 6: 517–528.
- Cometto, A., C. G. Ametrano, R. De Carolis, et al. 2024. "Highly Heterogeneous Mycobiota Shape Fungal Diversity in Two Globally Distributed Lichens." *Fungal Ecology* 69: 101331.
- Cometto, A., S. D. Leavitt, M. Grube, S. De Hoog, and L. Muggia. 2023. "Tackling Fungal Diversity in Lichen Symbioses: Molecular and Morphological Data Recognize New Lineages in Chaetothyriales (Eurotiomycetes, Ascomycota)." *Mycological Progress* 22, no. 8: 53.
- Conway, J. R., A. Lex, and N. Gehlenborg. 2017. "UpSetR: An R Package for the Visualization of Intersecting Sets and Their Properties." *Bioinformatics* 33, no. 18: 2938–2940.
- Cox, M. M., J. L. Keck, and J. R. Battista. 2010. "Rising From the Ashes: DNA Repair in *Deinococcus radiodurans*." *PLoS Genetics* 6, no. 1: e1000815.
- Crowther, T. W., D. S. Maynard, T. R. Crowther, J. Peccia, J. R. Smith, and M. A. Bradford. 2014. "Untangling the Fungal Niche: The Trait-Based Approach." *Frontiers in Microbiology* 5: 579.
- de León, L. R., T. Moreno-Perlín, T. Castillo-Marengo, et al. 2025. "Polyextremotolerant, Opportunistic, and Melanin-Driven Resilient Black Yeast *Exophiala dermatitidis* in Environmental and Clinical Contexts." *Scientific Reports* 15, no. 1: 6472.
- Egidi, E., G. S. de Hoog, D. Isola, et al. 2014. "Phylogeny and Taxonomy of Meristematic Rock-Inhabiting Black Fungi in the Dothideomycetes Based on Multi-Locus Phylogenies." *Fungal Diversity* 65: 127–165.
- Egidi, E., M. Delgado-Baquerizo, J. M. Plett, et al. 2019. "A Few Ascomycota Taxa Dominate Soil Fungal Communities Worldwide." *Nature Communications* 10, no. 1: 2369.
- Emms, D. M., and S. Kelly. 2019. "OrthoFinder: Phylogenetic Orthology Inference for Comparative Genomics." *Genome Biology* 20, no. 1: 238.
- Fick, S. E., and R. J. Hijmans. 2017. "WorldClim 2: New 1-Km Spatial Resolution Climate Surfaces for Global Land Areas." *International Journal of Climatology* 37, no. 12: 4302–4315.
- Fu, C., A. Davy, S. Holmes, et al. 2021. "Dynamic Genome Plasticity During Unisexual Reproduction in the Human Fungal Pathogen *Cryptococcus Deneoformans*." *PLoS Genetics* 17, no. 11: e1009935.
- Gomez-Gutierrez, S. V., W. R. Sic-Hernandez, S. Haridas, et al. 2024. "Comparative Genomics of the Extremophile *Cryomyces antarcticus* and Other Psychrophilic Dothideomycetes." *Frontiers in Fungal Biology* 5: 1418145.
- Gonçalves, A. P., J. Heller, A. Daskalov, A. Videira, and N. L. Glass. 2017. "Regulated Forms of Cell Death in Fungi." *Frontiers in Microbiology* 8: 1837.
- Gostinčar, C., C. Coleine, N. Gunde-Cimerman, and J. E. Stajich. 2024. "Fungi From Extreme Environments: Genome Sequences and Beyond." In *Fungal Genomics*, 33–48. Springer Nature Switzerland.
- Gostinčar, C., J. E. Stajich, A. Kežžar, et al. 2021. "Seven Years at High Salinity—Experimental Evolution of the Extremely Halotolerant Black Yeast *Hortaea werneckii*." *Journal of Fungi* 7, no. 9: 723.
- Gueidan, C., C. Ruibal, G. S. De Hoog, and H. Schneider. 2011. "Rock-Inhabiting Fungi Originated During Periods of Dry Climate in the Late Devonian and Middle Triassic." *Fungal Biology* 115, no. 10: 987–996.
- Haas, B. J., S. L. Salzberg, W. Zhu, et al. 2008. "Automated Eukaryotic Gene Structure Annotation Using EVIDENCEModeler and the Program to Assemble Spliced Alignments." *Genome Biology* 9, no. 1: R7.
- Harder, C. B., S. Miyauchi, M. Virágh, et al. 2024. "Extreme Overall Mushroom Genome Expansion in *Mycena* ss Irrespective of Plant Hosts or Substrate Specializations." *Cell Genomics* 4, no. 7: 1–16.
- Hardwick, J. M. 2018. "Do Fungi Undergo Apoptosis-Like Programmed Cell Death?" *MBio* 9, no. 4: 10–1128.
- Hijmans, R. J. 2023. "raster: Geographic Data Analysis and Modeling. R Package Version, 3, 6." <https://cran.r-project.org/web/packages/raster/raster.pdf>.

- Huerta-Cepas, J., K. Forslund, L. P. Coelho, et al. 2017. "Fast Genome-Wide Functional Annotation Through Orthology Assignment by eggNOG-Mapper." *Molecular Biology and Evolution* 34, no. 8: 2115–2122.
- Huson, D. H., D. C. Richter, C. Rausch, T. DeZulian, M. Franz, and R. Rupp. 2007. "Dendroscope: An Interactive Viewer for Large Phylogenetic Trees." *BMC Bioinformatics* 8: 1–6.
- Kanehisa, M., S. Goto, Y. Sato, M. Kawashima, M. Furumichi, and M. Tanabe. 2014. "Data, Information, Knowledge and Principle: Back to Metabolism in KEGG." *Nucleic Acids Research* 42, no. D1: D199–D205.
- Kassambara, A., and F. Mundt. 2020. "Factoextra: Extract and Visualize the Results of Multivariate Data Analyses." R Package Version 1.0.7.
- Korf, I. 2004. "Gene Finding in Novel Genomes." *BMC Bioinformatics* 5, no. 1: 59.
- Leff, J. W., S. E. Jones, S. M. Prober, et al. 2015. "Consistent Responses of Soil Microbial Communities to Elevated Nutrient Inputs in Grasslands Across the Globe." *Proceedings of the National Academy of Sciences* 112, no. 35: 10967–10972.
- Lenassi, M., C. Gostinčar, S. Jackman, et al. 2013. "Whole Genome Duplication and Enrichment of Metal Cation Transporters Revealed by De Novo Genome Sequencing of Extremely Halotolerant Black Yeast *Hortaea werneckii*." *PLoS One* 8, no. 8: e71328.
- Li, C., X. Zhang, T. Ye, X. Li, and G. Wang. 2022. "Protection and Damage Repair Mechanisms Contributed to the Survival of *Chroococciopsis* sp. Exposed to a Mars-Like Near Space Environment." *Microbiology Spectrum* 10, no. 6: e03440-22.
- Liaw, A., and M. Wiener. 2002. "Classification and Regression by randomForest." *R News* 2, no. 3: 18–22.
- Liu, C., Y. Cui, X. Li, and M. Yao. 2021. "Microeco: An R Package for Data Mining in Microbial Community Ecology." *FEMS Microbiology Ecology* 97, no. 2: fiaa255.
- Majoros, W. H., M. Pertea, and S. L. Salzberg. 2004. "TigrScan and GlimmerHMM: Two Open Source Ab Initio Eukaryotic Gene-Finders." *Bioinformatics* 20, no. 16: 2878–2879.
- Mallavan, B. P., B. Minasny, and A. B. McBratney. 2010. "Homosoil, a Methodology for Quantitative Extrapolation of Soil Information Across the Globe." In *Digital Soil Mapping*, 137–150. Springer.
- Manni, M., M. R. Berkeley, M. Seppey, and E. M. Zdobnov. 2021. "BUSCO: Assessing Genomic Data Quality and Beyond." *Current Protocols* 1, no. 12: e323.
- Martiny, J. B. H., S. E. Jones, J. T. Lennon, and A. C. Martiny. 2015. "Microbiomes in Light of Traits: A Phylogenetic Perspective." *Science* 350: aac9323.
- McMurdie, P. J., and S. Holmes. 2013. "Phyloseq: An R Package for Reproducible Interactive Analysis and Graphics of Microbiome Census Data." *PLoS One* 8, no. 4: e61217.
- Minkin, I., and P. Medvedev. 2020. "Scalable Multiple Whole-Genome Alignment and Locally Collinear Block Construction With SibeliaZ." *Nature Communications* 11: 6327.
- Napoli, A., F. Iacovelli, C. Fagliarone, G. Pascarella, M. Falconi, and D. Billi. 2021. "Genome-Wide Identification and Bioinformatics Characterization of Superoxide Dismutases in the Desiccation-Tolerant Cyanobacterium *Chroococciopsis* sp. CCME 029." *Frontiers in Microbiology* 12: 660050.
- Nguyen, L. T., H. A. Schmidt, A. von Haeseler, and B. Q. Minh. 2015. "IQ-TREE: A Fast and Effective Stochastic Algorithm for Estimating Maximum Likelihood Phylogenies." *Molecular Biology and Evolution* 32: 268–274.
- Palmer, J. M., and J. E. Stajich. 2022. "Automatic Assembly for the Fungi (AAFTF): Genome Assembly Pipeline."
- Piñeiro, G., S. Perelman, J. P. Guerschman, and J. M. Paruelo. 2008. "How to Evaluate Models: Observed vs. Predicted or Predicted vs. Observed?" *Ecological Modelling* 216: 316–322.
- Purahong, W., T. Arnstadt, T. Kahl, et al. 2016. "Are Correlations Between Deadwood Fungal Community Structure, Wood Physico-Chemical Properties and Lignin-Modifying Enzymes Stable Across Different Geographical Regions?" *Fungal Ecology* 22: 98–105.
- Rampelotto, P. H. 2010. "Resistance of Microorganisms to Extreme Environmental Conditions and Its Contribution to Astrobiology." *Sustainability* 2, no. 6: 1602–1623.
- Rice, P., I. Longden, and A. Bleasby. 2000. "EMBOSS: The European Molecular Biology Open Software Suite." *Trends in Genetics* 16, no. 6: 276–277.
- Rillig, M. C., M. G. Van der Heijden, M. Berdugo, et al. 2023. "Increasing the Number of Stressors Reduces Soil Ecosystem Services Worldwide." *Nature Climate Change* 13, no. 5: 478–483.
- Rosling, A., I. Timling, and D. L. Taylor. 2013. "Archaeorhizomycetes: Patterns of Distribution and Abundance in Soil." In *Genomics of Soil- and Plant-Associated Fungi*, 333–349. Springer.
- Sato, M., M. Suda, J. Okuma, et al. 2017. "Isolation of Highly Thermostable  $\beta$ -Xylosidases From a Hot Spring Soil Microbial Community Using a Metagenomic Approach." *DNA Research* 24, no. 6: 649–656.
- Schultz, J., A. dos Santos, N. Patel, and A. S. Rosado. 2023. "Life on the Edge: Bioprospecting Extremophiles for Astrobiology." *Journal of the Indian Institute of Science* 103, no. 3: 721–737.
- Sinha, S., S. Flibotte, M. Neira, et al. 2017. "Insight Into the Recent Genome Duplication of the Halophilic Yeast *Hortaea werneckii*: Combining an Improved Genome With Gene Expression and Chromatin Structure." *G3: Genes, Genomes, Genetics* 7, no. 7: 2015–2022.
- Slade, D., A. B. Lindner, G. Paul, and M. Radman. 2009. "Recombination and Replication in DNA Repair of Heavily Irradiated *Deinococcus radiodurans*." *Cell* 136, no. 6: 1044–1055.
- Smith, M. R. 2020. "TreeDist: Distances Between Phylogenetic Trees." R Package Version 2.9.2. <https://doi.org/10.5281/zenodo.3528124>.
- Sterflinger, K., D. Tesei, and K. Zakharova. 2012. "Fungi in Hot and Cold Deserts With Particular Reference to Microcolonial Fungi." *Fungal Ecology* 5, no. 4: 453–462.
- Tedersoo, L., M. Bahram, S. Pölme, et al. 2014. "Global Diversity and Geography of Soil Fungi." *Science* 346, no. 6213: 1256688.
- Tedersoo, L., V. Mikryukov, S. Anslan, et al. 2021. "The Global Soil Mycobiome Consortium Dataset for Boosting Fungal Diversity Research." *Fungal Diversity* 111, no. 1: 573–588.
- Vafadarnejad, E., M. A. Amoozgar, J. Khansha, and R. Fallahzade. 2015. "The rad2 Gene of Haloarchaeum *Halobacterium salinarum* Is Functional in the Repair of Ultraviolet Light Induced DNA Photoproducts." *Microbiological Research* 173: 44–49.
- Vande Zande, P., X. Zhou, and A. Selmecki. 2023. "The Dynamic Fungal Genome: Polyploidy, Aneuploidy and Copy Number Variation in Response to Stress." *Annual Review of Microbiology* 77, no. 1: 341–361.
- Zomer, R. J., J. Xu, and A. Trabucco. 2022. "Version 3 of the Global Aridity Index and Potential Evapotranspiration Database." *Scientific Data* 9: 409.

### Supporting Information

Additional supporting information can be found online in the Supporting Information section. **Table S1:** The table reports geographic coordinates (latitude, longitude), biome classification, climate descriptors, and environmental parameters including mean annual temperature (MAT), mean annual precipitation (MAP), aridity index (AI), potential evapotranspiration (PET), soil properties (pH, sand content, SOC), UV radiation, elevation, and human influence index (HII) for

each sampling location. **Table S2:** Operational taxonomic units (OTUs) are reported with their corresponding taxonomic classification from kingdom to species level, along with unique sequence identifiers and assigned phylotypes. **Table S3:** The table includes taxonomic identity, geographic origin, isolation source, and a comprehensive set of bioclimatic variables (BIO1–BIO19), solar radiation, UV index, and Köppen–Geiger climate classification (Beck\_KG\_V1), along with human influence index (HII). **Table S4:** Assembly metrics include contig number, total assembly length, contig size distribution (minimum, maximum, mean, median), N50/N90 and L50/L90 values, GC content, and BUSCO-based completeness estimates. **Table S5:** The table reports the abundance of KEGG orthologs (#term) for each genome, providing a quantitative overview of functional potential and metabolic pathway representation across isolates. **Table S6:** Orthogroups identified through comparative genomic analysis are reported along with gene counts per genome and total gene membership per orthogroup, enabling the identification of conserved and lineage-specific gene families.